Available online at www.sciencedirect.com

SCIENCE DIRECT®

Tectonophysics 395 (2005) 81–97

TECTONOPHYSICS

www.elsevier.com/locate/tecto

Deformation mode in the frontal edge of an arc–arc collision zone: subsurface geology, active faults and paleomagnetism in southern central Hokkaido, Japan

Yasuto Itoh[a,*], Tatsuya Ishiyama[b], Yasuhiko Nagasaki[c]

[a]*Department of Earth Sciences, College of Integrated Arts and Sciences, Osaka Prefecture University, Gakuen-cho 1-1, Sakai, Osaka 599-8531, Japan*
[b]*AIST - Geological Survey of Japan, Central 7th, Higashi 1-1-1, Tsukuba 305-8567, Japan*
[c]*Technical Department, Japan National Oil Corporation, Uchisaiwai-cho 2-2-2, Chiyoda-ku, Tokyo 100-8511, Japan*

Received 10 September 2003; accepted 6 September 2004

Abstract

Frontal edge of a Cenozoic arc–arc collision zone in southern central Hokkaido is described based on subsurface geology. Reflection seismic and drilling surveys delineate geologic structure of the N–S fold-and-thrust belt. West-verging faulted blocks extend as long as 200 km in central Hokkaido, and the activity of thrust has been propagating westward since the late Neogene. The Cretaceous paleomagnetic data obtained from cores and the affinity in basement lithology implies a connection between the downthrown block of a floor thrust of the collision front and paleo-northeast Japan arc. Remanent magnetization of core samples belonging to the upthrown block indicates post-Oligocene counterclockwise rotation. It is opposite to surface rotational motions of the same block, then more detail study on fault architecture and block rotation is required to understand the mode of deformation of the fold-and-thrust belt. Maturity level of organic matters in a borehole suggests that burial by the thrusting initiated in the Quaternary. Thus, the deformation front of the arc–arc collision is in an active, nascent stage of crustal contraction.

Keywords: Hokkaido; Arc–arc collision; Seismic interpretation; Borehole; Active fault; Paleomagnetism

1. Introduction

Southern central Hokkaido, northernmost component of the Japanese Islands (Fig. 1) has been a site of arc–arc collision events since the early Tertiary. The older collision between paleo-North American and Eurasian Plates initiated in the Eocene and resulted in metamorphism under the Hidaka Mountains (Komatsu et al., 1983, 1989). A right-lateral component of motion is postulated for the contractional event based on the fabric of metamorphic

* Corresponding author. Fax: +81 72 254 9752.
E-mail address: itoh@el.cias.osakafu-u.ac.jp (Y. Itoh).

0040-1951/$ - see front matter © 2004 Elsevier B.V. All rights reserved.
doi:10.1016/j.tecto.2004.09.003

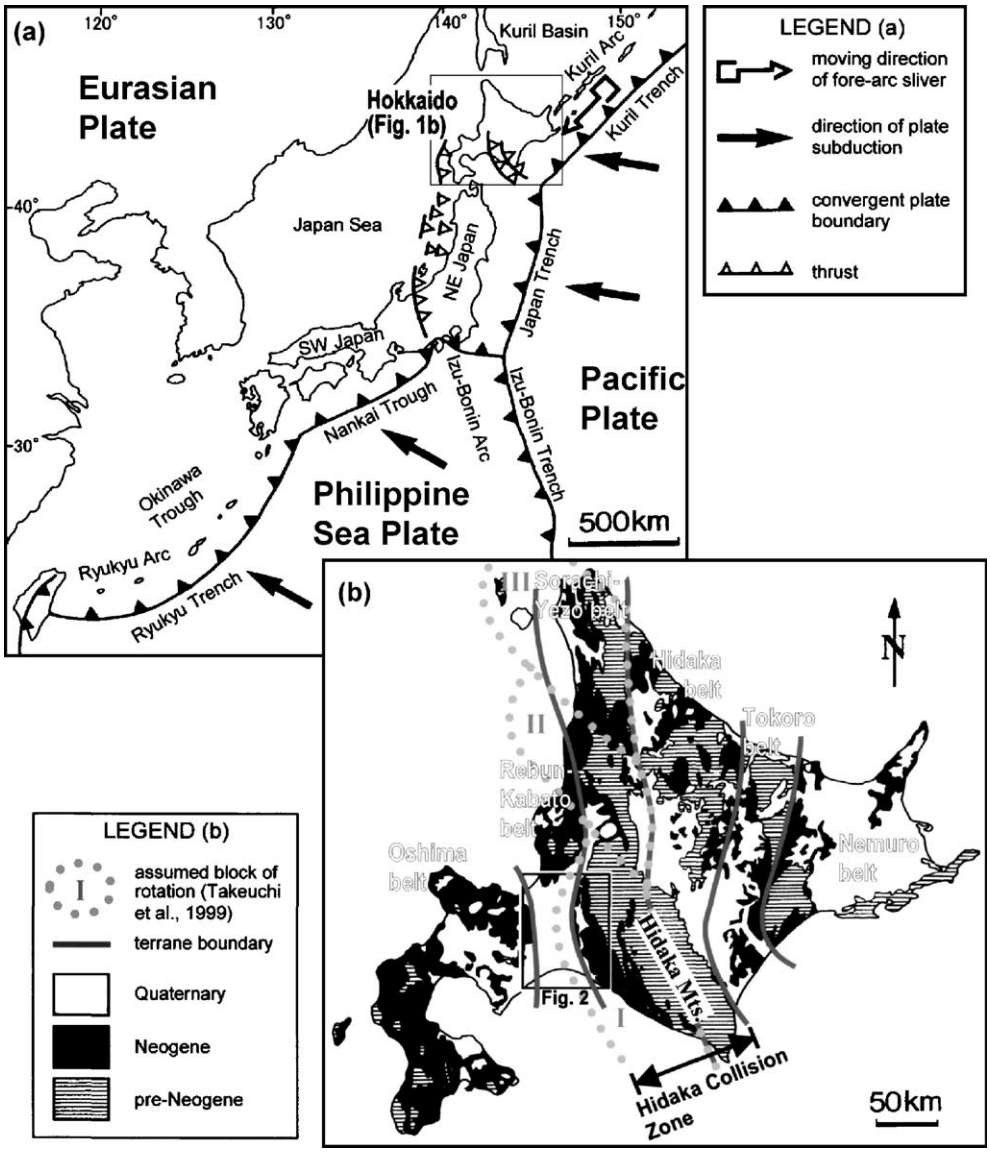

Fig. 1. Maps showing tectonic context around the Japanese Islands (a) and geologic belts in Hokkaido (b; after Kato et al., 1990).

rocks (Arita et al., 1986). The younger collision was caused by the westward migration of fore–arc sliver of the Kuril arc (Fig. 1) since the late Miocene (Kimura and Tamaki, 1985), which enhanced uplift of the Hidaka Mountains and resulted in crustal shortening of ~60 km (Kazuka et al., 2002). Between such events, Kuril and Japan back-arc basins began to spread (Lallemand and Jolivet, 1986) inevitably, raising rotation and rearrangement of the constituents of Hokkaido. Takeuchi et al. (1999) regarded central Hokkaido as blocks of clockwise rotation based on paleomagnetic research (Fig. 1b). Their hypothetical blocks, however, have not been verified through geologic structures indicative of shearing boundary or coherency of intra-block paleomagnetic directions.

Thus, a series of tectonic events along the eastern Eurasian margin and the formation process of

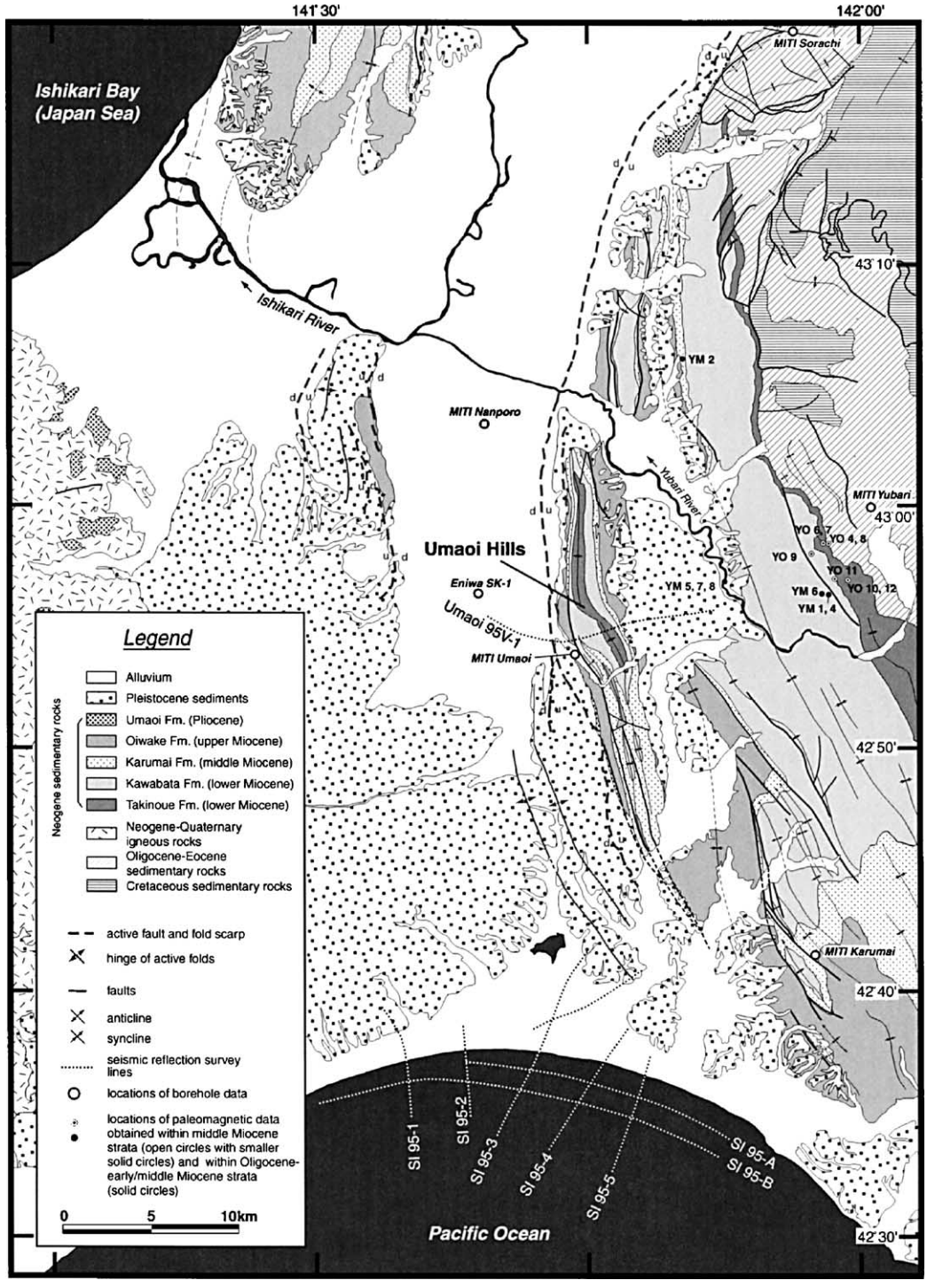

Fig. 2. Geologic map around the Umaoi anticline redrawn from Geological Survey of Japan (2002). Location of active fault and/or fold scarps (after Ikeda et al., 2002) are also shown. "u" and "d" attached on fault traces are upthrown and downthrown sides of faults, respectively. Sampling points of surface paleomagnetic data is after Kodama et al. (1993).

continental crust are recorded in the complex geologic features in central Hokkaido. In this article, the authors attempt to elucidate deformation mode within the western margin of the collision zone, around the Umaoi Hills (Fig. 2), where active reverse faulting is observed (Ikeda et al., 2002). It is interpreted as the nascent portion of the westward propagating crustal contraction (Ito, 2000). From another point of view, our study area belongs to the clockwise-rotated Block I (Fig. 1b) after Takeuchi et al. (1999). Based on subsurface information from seismic and drilling surveys, we delineate geologic structures beneath the collision front. Then, paleomagnetic analyses are executed on core samples obtained from boreholes in order to assess rotational motions around the fold-and-thrust belt. Because core recovery in case of exploration is quite low (generally less than 2%) unlike academic drilling (e.g., ODP), we have made an effort to obtain samples as much as possible. Notwithstanding low recovery rate of core samples, deep exploration drilling under mud circulation with physical properties continuously obtained through logging provides us with a unique information to clarify subsurface structure.

Our data require differential rotations within the collision zone (or the hypothetical coherent block), suggesting complicated modes of deformation. Finally, degrees of organic maturation of borehole samples are simulated using a kinetic model. The result gives us an estimate for the duration of thrust activity on the active collision front.

2. Background

2.1. Geology

Fig. 2 summarizes geologic units (Kato et al., 1990; Geological Survey of Japan, 2002) and faults around the study area. Umaoi Hills exist along western margin of the Hidaka Collision Zone. It consists of faulted anticlines of the Neogene rocks with narrow (under mappable size) exposures of the Oligocene Minami-naganuma Formation (Kurita and Yokoi, 2000), which thickly develops beneath the Umaoi Hills and Ishikari lowland. Divided by an active thrust, Ishikari lowland on the west of collision zone is covered by thick sedimentation. In an attempt to find hydrocarbon reserves, numerous seismic and drilling surveys have been organized in the area (Ishiwada et al., 1992). Important drilling sites and seismic lines interpreted in this article are shown in Fig. 2.

We adopted two boreholes for geologic and paleomagnetic analyses. MITI Umaoi (UM) was drilled on the Umaoi Hills, and penetrated thrust sheets of the Paleogene units. In this study, paleomagnetic results for the Paleogene Minami-naganuma Formation and the igneous basement samples beneath the floor thrust will be presented in the following sections. Eniwa SK-1 (EN) was drilled in the Ishikari lowland and reached the earliest Cretaceous volcanic/sedimentary complex (Suzuki et al., 1999). We collected samples from the Cretaceous sedimentary rocks, of which directional markers (bedding plane, fracture) are available to determine core orientation and attitude of tectonic tilt.

2.2. Active faults

From a standpoint of tectonic geomorphology, the Umaoi Hills are a geomorphic expression of active folding at the leading edge of the fold-and-thrust belt along the western margin of the Hidaka Collision Zone. Recent deformations of the Umaoi Hills are recorded in flights of fluvial and marine terraces approximately correlated with marine isotope stage of 5 and 7 (Koike and Machida, 2001) that cover western flank of an anticline (Fig. 2; Ikeda et al., 2002). Numerous flexural slip faults that cut and deform the terraces also suggest that a strong contraction occurs within forelimb of the anticline beneath the hills. Pyroclastic flow deposits at 40–42 ka, which mantle the southern Umaoi Hills, are also incorporated in structural growth of the anticline (Ikeda et al., 2002). In addition, fold scarps and active folds upon the depositional surfaces of the pyroclastic flow are continuously traced about 5 km to the west of the southern Umaoi Hills (Ikeda et al., 2002), indicating that pairs of imbricate thrusting occur at the leading edge during the late Pleistocene time.

3. Seismic interpretation

3.1. Umaoi section

Fig. 3 shows a multichannel E–W seismic profile across the Umaoi Hills. In 1995, a seismic survey was conducted by JAPEX. During the shooting, 330 channels of geophones (with an interval of 25 m) recorded the energy released from six vibrators, shot at 50-m interval. Raw seismic data were stacked and then subjected to a poststack processing sequence in order to enhance the resolution.

MITI Umaoi and some exploration boreholes have been drilled upon or near this seismic line, and their geologic data (JNOC, 1997) provide important constraints on an interpretation. As stated by Kurita and Yokoi (2000), the N–S trending hills are intensively folded and faulted with westward vergence. Thrust blocks and their internal geologic structure were confirmed as repeated Paleogene sections and attitude of bedding planes within the MITI Umaoi (Kurita and Yokoi, 2000; JNOC, 1997), respectively. The floor thrust coincides with a boundary between the tilted thrust horses and flat-lying horst-graben of the Paleogene and Cretaceous igneous basement.

It is noteworthy that the Neogene/Quaternary on western flank of the anticlinal form are clearly deformed, suggesting thrust activity until recent period. Ages of such growth strata provide a clue to reconstruct history of fault motion and tectonic events, thus will be examined in Discussion section. On the other hand, the middle Miocene Kawabata Formation on the eastern flank is involved into fault–bend fold, and truncated by the Karumai Formation in the late Miocene. Although the east-dipping fault in the eastern part of the section cuts the Karumai Formation, the flat-lying strata imply that fault activity in the eastern area declined in late Neogene. Therefore, thrusts bounding the Hidaka Collision Zone seem to propagate westward through the long-standing collision event as suggested by Ito (2000).

3.2. Southern offshore section

Fig. 4 shows a multichannel E–W seismic profile along the southern coast of central Hokkaido where economic reserves of hydrocarbon were confirmed and numerous boreholes have been drilled to clarify subsurface geologic structure (Kurita and Yokoi, 2000; Ishiwada et al., 1992; Taketomi and Nishita, 2002). In 1995, a seismic survey was conducted around the coastal area by Ministry of Economy, Trade and Industry, (METI) Japan (JNOC, 1996). During the shooting, 80 channels of hydrophones (with an interval of 25 m) recorded the energy released from a 24.6 l (1500 in^3) tuned airgun array, shot at 25-m interval. Raw seismic data were stacked and then subjected to a post-stack processing sequence in order to enhance the resolution. The SI 95-A seismic profile transects the southward projection of pairs of active folds around the Umaoi Hills.

Interpretation of the section (JNOC, 1996) shows that the seismic data successfully images pairs of west-verging anticlines. These folds are underlain by a west-verging thrust with shallow dips that crosscuts the early Miocene strata (Takinoue Formation). Uniform thickness of the Karumai Formation in late Miocene throughout the seismic section, identified by continuous reflectors, indicates that the Miocene strata predate the essential structural growth of the folds and are involved in hangingwall blocks.

Tabular beds of pregrowth (late Miocene–Pliocene) formations are overlain by the Quaternary strata that taper hindward and onlap onto forelimbs and backlimbs. These geometric relationships suggest that the Quaternary has buried structural relief of the underlying formations, and has been folded and rotated during their deposition. Hence, growth (Quaternary) strata juxtaposed with either forelimbs or backlimbs indicate structural growth of active folds during the Quaternary.

3.3. Active thrusting related to arc–arc collision

The present seismic interpretation demonstrates that a N–S thrust has been activated through the late Cenozoic bounding the western margin of the Hidaka Collision Zone. To the north, active landforms of the thrust can be traced as far as 43°30′N (Ikeda et al., 2002). Southern extension of the thrust is identified as the deformation front of offshore fold zone (Ito, 2000) as far as 42°N. Therefore, the tectonic boundary is at least 200-km long, and comparable with width of the Kuril fore–arc sliver (Kimura, 1996) colliding against the continental lithosphere of Hokkaido. A series of microearthquake observations (Katsumata et al.,

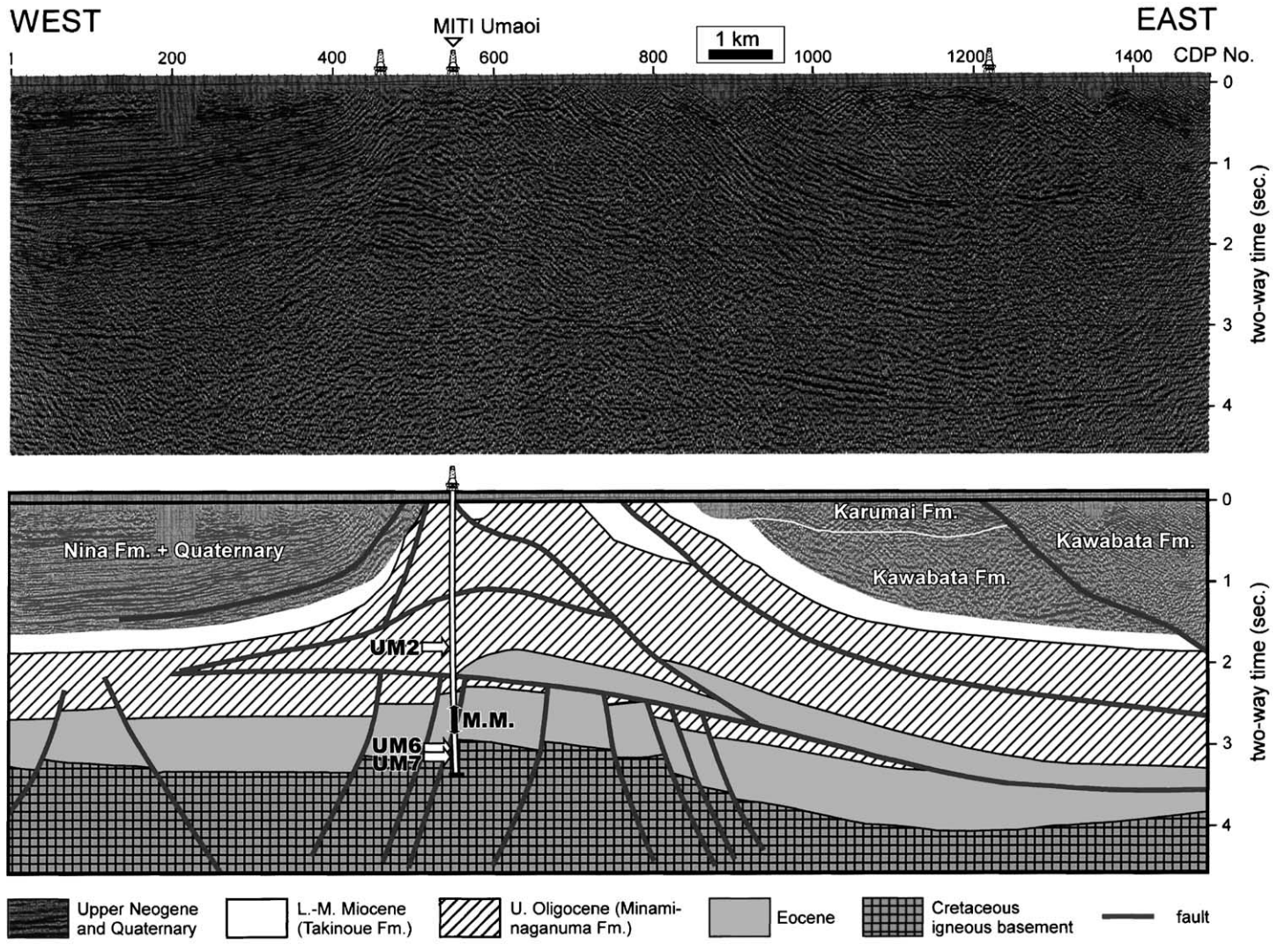

Fig. 3. E–W multichannel seismic profile 95V-1 (migrated; upper) and its geologic interpretation (lower) running near the MITI Umaoi (at CDP no.550). Subsurface fault architecture and unit boundaries are based on interpretation of the exploration drilling (JNOC, 1997; Kurita and Yokoi, 2000). Paleomagnetic sampling horizons (UM2, 6, 7) are shown on the projected trace of the MITI Umaoi after depth to time conversion. Interval of maturity modeling (MM) is also shown on the same profile. See Fig. 2 for seismic line location.

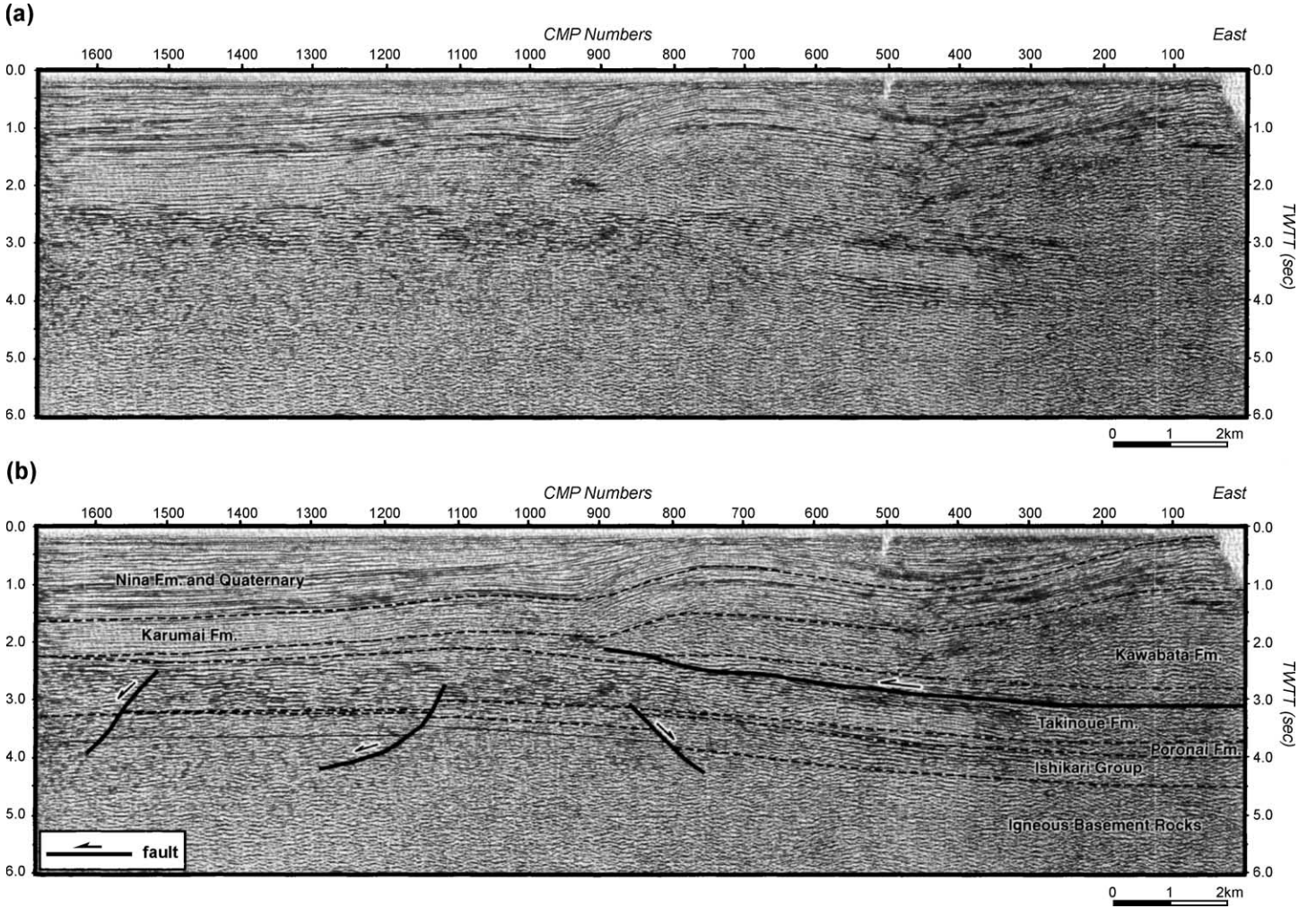

Fig. 4. E–W multichannel seismic profile SI95-A (migrated; upper) and its geologic interpretation (lower) along the coast of southern central Hokkaido. Subsurface unit boundaries are after JNOC (1996). See Fig. 2 for seismic line location.

2002) showed that thrust-type focal mechanism was dominant around our study area. In order to assess the future development of the arc–arc collision, deformation history of the active and nascent fold-and-thrust belt is of great importance.

4. Paleomagnetism

Core samples for paleomagnetic analyses were obtained from the Eniwa SK-1 and MITI Umaoi boreholes, both of which had been drilled nearly vertically. Although core recovery intervals of these wells aimed at hydrocarbon exploration were quite short, subsurface samples with structural information provide us with an opportunity to study three-dimensional rotation scheme. Sampling depth, lithology and geologic ages (Kurita and Yokoi, 2000; Suzuki et al., 1999; JNOC, 1997) are summarized in Table 1. As for the MITI Umaoi borehole, sampling depths are converted to two-way travel time based on vertical seismic profiling (VSP), and shown on the interpreted profile in Fig. 3.

4.1. Sample preparation

All samples of the Eniwa SK-1 and the Oligocene samples (UM2-1~6) of the MITI Umaoi were successfully oriented based on correlation between directional markers (bedding plane and fracture) on core surfaces and side-wall images by borehole logging. Fracture patterns upon the Eniwa SK-1 cores were identical with those appeared on the logging images. The Oligocene core samples (UM2-1~6) of the MITI Umaoi show rather wide ranges of dip angles (20~44°), which is comparable with those of logging data (28~47°). Because the dipping directions around the sampling interval are quite constant (289~291°), cores can be oriented with high reliability. As for the Cretaceous igneous rocks (UM6, 7) of the MITI Umaoi well, samples were not initially oriented because sidewall imaging data were not available. Cylindrical rock specimens for magnetic measurements of 25 mm in diameter and 22 mm in length were cut from the core samples avoiding areas with dense fracture or serious alteration.

Bulk magnetic susceptibility was measured for all specimens using a Bartington susceptibility meter (MS2). Natural remanent magnetizations (NRM) of all specimens were measured with a 2-G Enterprise three-axis cryogenic magnetometer or a spinner magnetometer (Natsuhara-Giken SMM-85) settled in a magnetically shielded laboratory at Kyoto University.

4.2. Demagnetization test

We conducted progressive thermal demagnetization (PThD) test in order to isolate stable components of remanent magnetization. PThD test was performed, up to 690 °C in air, using a non-inductively wound electric furnace with an internal residual magnetic field less than 10 nT. Demagnetization was interrupted when specimens were broken into numerous pieces because of repeated heating and cooling procedures.

Table 1
Description of core samples obtained from the southern central Hokkaido

Well name	Core	Depth (m)	ID (core-horizon)	Lithology (Formation)	*N*	Age (method)
Eniwa SK-1	1	4577.71–0.78	EN1-1	mudstone	3	143–141 Ma (radiolaria)
	1	4577.89–0.96	EN1-2	mudstone	7	143–141 Ma (radiolaria)
MITI Umaoi	2	2377.28–0.48	UM2-1	siltstone (Minami-naganuma)	12	L. Oligocene (dinoflagellate)
	2	2378.60–0.80	UM2-2	siltstone (Minami-naganuma)	11	L. Oligocene (dinoflagellate)
	2	2379.20–0.40	UM2-3	siltstone (Minami-naganuma)	12	L. Oligocene (dinoflagellate)
	2	2380.30–0.50	UM2-4	siltstone (Minami-naganuma)	9	L. Oligocene (dinoflagellate)
	2	2381.68–0.88	UM2-5	siltstone (Minami-naganuma)	9	L. Oligocene (dinoflagellate)
	2	2383.08–0.26	UM2-6	siltstone (Minami-naganuma)	12	L. Oligocene (dinoflagellate)
	6	4851.56–0.63	UM6-1	gabbro	3	102, 101 Ma (K-Ar)
	7	5018.27–0.37	UM7-1	gabbro	1	128 Ma (K-Ar); 95 Ma (FT)
	7	5018.41–0.51	UM7-2	gabbro	5	128 Ma (K-Ar); 95 Ma (FT)

N is number of specimens for paleomagnetic measurements.

Fig. 5 shows typical results of PThD for the MITI Umaoi Oligocene sedimentary rocks. Some horizons (a) are characterized by overlapping T_{UB} spectra of primary and secondary components, then remagnetization circle fitting (McFadden and McElhinny, 1988) was adopted to determine directions of characteristic remanent magnetization (ChRM). Other horizons (b) had univectorial demagnetization trend apart from recent geomagnetic field direction, then principal component analysis (Kirschvink, 1980) was adopted for ChRM calculation. As a result, we obtained four normal and reversed mean directions for the Late Oligocene Minami-naganuma Formation (Fig. 5c, Table 2). All of them are characterized by counterclockwise deflection in declinations after tilt-correction.

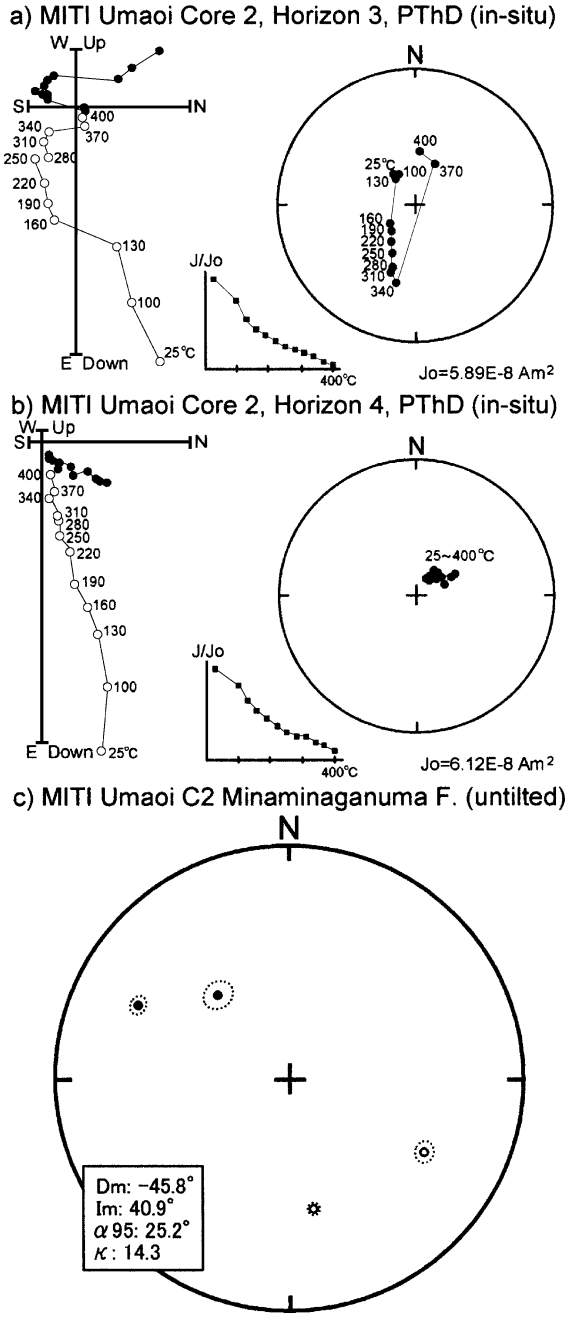

Fig. 5. (a, b) Results of progressive thermal demagnetization (PThD) for the Late Oligocene core samples in the MITI Umaoi borehole. Directional data are shown up to 400 °C because these samples became quite unstable and acquired secondary remanent magnetization after higher levels of PThD. Vector-demagnetization diagrams are drawn on the left. Unit of the coordinates is bulk remanent intensity. Solid and open circles are projections of vector end-points on the horizontal and N–S vertical planes, respectively. Equal-area projections and normalized intensity decay curves are on the right. (●) Plotted on the lower hemisphere of the projections. Numbers attached on the symbols depict levels of PThD in degrees Celsius. (c) Untilted characteristic mean directions from four horizons have westerly deflection in declinations. Solid and open circles are plotted on the lower and upper hemispheres of the projection, respectively. Dotted ovals are 95% confidence limits.

Fig. 6 presents typical results of PThD for the Cretaceous rocks of the Eniwa SK-1 and MITI Umaoi. Reddish mudstones from the Eniwa SK-1 (EN-series) preserve three distinct components of NRM. A high-temperature component (600<unblocking temperatures (T_{UB})<690 °C) with easterly reversed directions was isolated, as was an intermediate-temperature component (400<T_{UB}<580 °C) with westerly normal directions. A low-temperature component (150<T_{UB}<400 °C) was identified, and its northerly direction similar to that of the present geomagnetic field suggests that the component is originated from thermoviscous remanent magnetization (TVRM) acquired during the latest Brunhes normal polarity chron.

Two distinct components were isolated from NRM of the MITI Umaoi gabbro samples (Fig. 6b; UM-series). A high-temperature component (520<T_{UB}<580 °C) with shallow inclinations was isolated, whereas a low-temperature component (150<T_{UB}<500 °C) with normal inclinations was identified. As mentioned before, cores of this borehole were not initially oriented, thus origin of

Table 2
Paleomagnetic directions of the Minami-naganuma Formation in MITI Umaoi, southern central Hokkaido

Horizon	Facies	Method	DMG (°C)	D (°)	I (°)	Dc (°)	Ic (°)	α_{95} (°)	κ	N	ϕ	λ
UM2-2	siltstone	RC	100–340	−158.2	−50.1	170.3	−42.4	2.1	960.2	8	70.0	−11.7
UM2-3	siltstone	RC	100–340	138.2	−74.7	118.8	−35.1	3.4	367.5	8	34.0	47.1
UM2-4	siltstone	PCA	130–400	34.7	70.9	−40.4	50.1	4.9	128.2	8	55.9	44.7
UM2-5	siltstone	PCA	130–420	−53.5	71.1	−64.0	27.7	2.9	373.0	8	28.9	45.0

RC and PCA are the remagnetization circle and principal component analysis, respectively, for determination of the mean directions. DMG is demagnetization range for calculation by RC/PCA method; D and I are in situ site-mean declination and inclination, respectively; Dc and Ic are untilted site-mean declination and inclination, respectively; α_{95} is radius of 95% confidence circle; κ is the Fisherian precision parameter; N is number of specimens; ϕ and λ are latitude (N) and longitude (E) of virtual geomagnetic poles for untilted site-mean directions, respectively.

the NRM components will be discussed in Section 4.4 based upon magnetic mineralogy described in the next section.

4.3. Magnetic mineralogy of the Cretaceous samples

In order to identify ferrimagnetic minerals of the Cretaceous samples characterized by multicomponent remanence, stepwise acquisition experiment of isothermal remanent magnetization (IRM) was performed on AF-demagnetized specimens in direct magnetic fields up to 2 T (Fig. 7a). As for the specimen from Eniwa SK-1 (EN), IRM intensity is characterized by initial rapid increase and gradual acquisition up to 2 T, indicating presence of magnetite and a high-coercivity mineral. On the other hand, IRM intensity of the specimen from MITI Umaoi (UM) almost saturates in applied fields lower than 0.2 T, and magnetite is the dominant contributor of stable remanent magnetization.

Next, we executed PThD of composite IRMs for the same specimens. Based on the procedure proposed by Lowrie (1990), composite IRMs were imparted by applying direct magnetic fields of 2, 0.4 and then 0.12 T onto the specimens in three orthogonal directions. As for the specimen from Eniwa SK-1 (EN1), decay curve of the IRM components through PThD test (see Fig. 7b) indicates that the dominant magnetic phase is the high (2~0.4 T) coercivity fraction with broad spectrum of T_{UB} up to 680 °C. Hence, carrier of the high-temperature component of NRM is hematite. Both medium (0.4~0.12 T) and soft (<0.12 T) coercivity fractions of less amount are identified, and we interpret that the fractions are mainly carried by larger (MD-size) grains of hematite because they have T_{UB} spectra up to 680 °C. As for the specimen from MITI Umaoi (UM6), soft coercivity fraction (<0.12 T) with T_{UB} spectrum up to 580 °C is dominant. Hence, the stable primary NRM is to be solely carried by titanomagnetite.

4.4. Origin and correction of NRM components of the Cretaceous samples

We determined the direction of each magnetic component using a three-dimensional least squares analysis technique (Kirschvink, 1980). Fig. 8 presents mean directions of isolated NRM components. As for the Eniwa SK-1 (EN), high- and intermediate-temperature components are nearly antipodal, showing counterclockwise deflections in declinations. Because the sample consists of reddish siliceous mudstone deposited in deep marine environment, high-temperature component carried by hematite may be post-depositional and prefolding magnetization as previously reported for cherts on the Eurasian margin (Oda and Suzuki, 2000; Shibuya and Sasajima, 1986). Thus, we adopt untilted direction of the high-temperature component for the tectonic discussion.

Because low-temperature component of the MITI Umaoi (UM) is characterized by inclination consistent with that of Earth's dipole field (62°) at the site latitude, we assume that the component is recent TVRM in origin and has in-situ northerly declination. This assumption is supported by the IRM experiments, showing that magnetite is the sole contributor for stable NRM components. As depicted in Fig. 9, theoretical contour for thermoviscous remagnetization for magnetite (Walton, 1980; Middleton and Schmidt, 1982) indicates that natural heating at ~150 °C, which is estimated by temperature logging (BHT), for duration of $\sim 10^6$ years, approximately corresponds

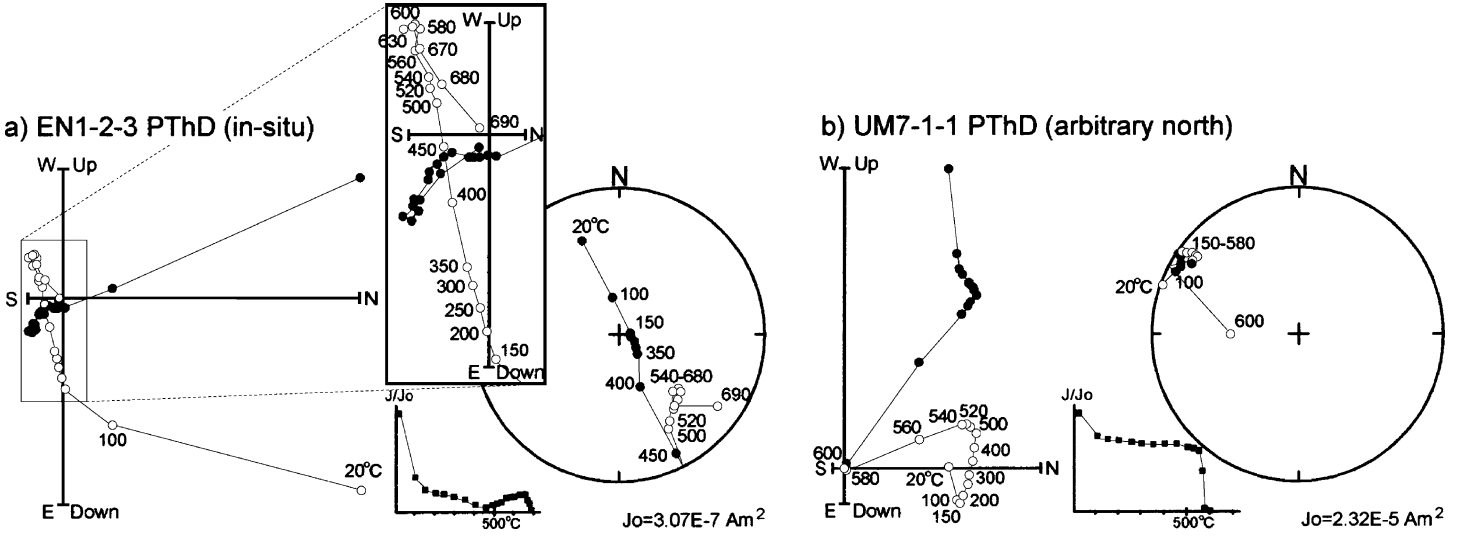

Fig. 6. Results of progressive thermal demagnetization (PThD) for the Cretaceous core samples in the Eniwa SK-1 (a) and MITI Umaoi (b) boreholes. Vector-demagnetization diagrams are drawn on the left. Unit of the coordinates is bulk remanent intensity. Solid and open circles are projections of vector end-points on the horizontal and vertical planes, respectively. Vertical planes are in N–S and arbitrary directions for the Eniwa SK-1 and MITI Umaoi, respectively. Equal-area projections and normalized intensity decay curves are on the right. Solid and open circles are plotted on the lower and upper hemispheres of the projections, respectively. Numbers attached on the symbols depict levels of PThD in degrees Celsius.

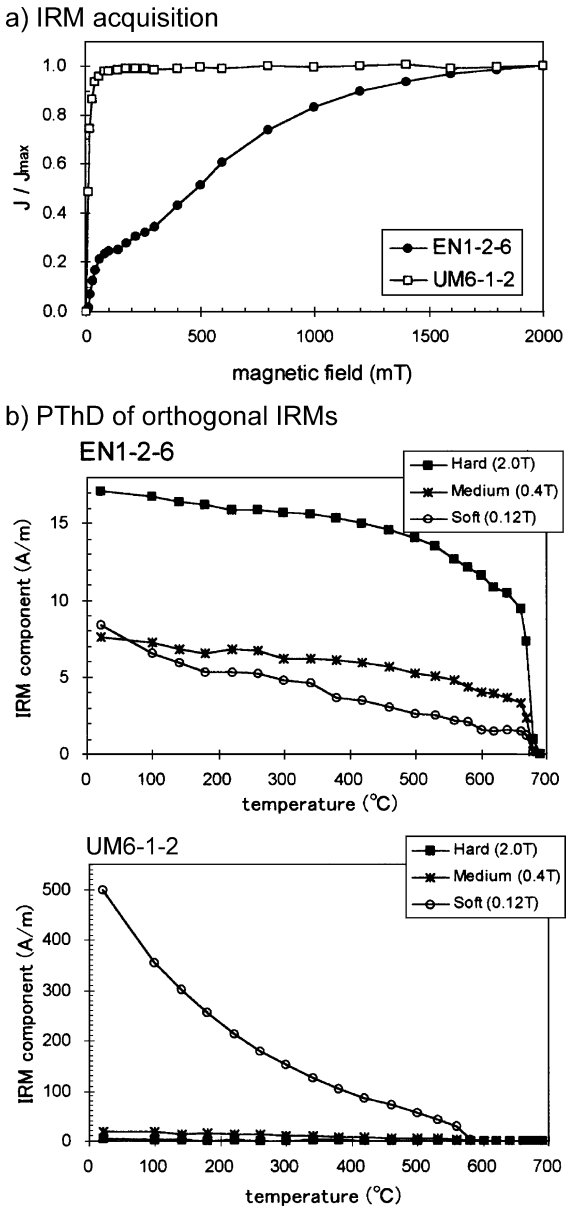

Fig. 7. (a) Progressive acquisition of isothermal remanent magnetization (IRM) for core samples in the Eniwa SK-1 (EN) and MITI Umaoi (UM) boreholes. (b) Thermal demagnetization curves of orthogonal IRMs for samples in the Eniwa SK-1 (upper) and MITI Umaoi (lower) boreholes.

to maximum T_{UB} ranges of the low-temperature component in laboratory. On such ground, the high-temperature component is converted into in-situ coordinates (Fig. 8e, e′). Shallow reversed inclination and counterclockwise deflection characterize the oriented directions of this component. As the sample was taken from a basement block with gentle dips on the seismic record (Fig. 3), the in situ direction is adopted for the tectonic discussion.

5. Discussion

Mean directions of the ChRM components of the studied two boreholes are listed in Table 3 together with surface paleomagnetic data obtained from southern central Hokkaido (Kodama et al., 1993). Although core samples obtained from deep drilling may have suffered drilling-induced remagnetization (Kikawa, 1993), our data do not show high inclination values (~80°) suggestive of such secondary origin. Therefore, we regard that the paleomagnetic data are immune from drilling disturbance in the following discussion. In order to understand evolution of the deformation front, we argue tectonic implication of the paleomagnetic information and an organic maturity modeling (MM) of borehole samples in the following sections.

5.1. Extent of the Cretaceous volcanic arc and its rotational motion

Basement rocks of the MITI Umaoi consist of gabbro and metabasalt, which are correlated with igneous Kumaneshiri Group in the Rebun–Kabato belt (Fig. 1; Kato et al., 1990). As the igneous rocks show geochemical affinity with arc–volcanism (Nagata et al., 1986; Ikeda and Komatsu, 1986), distribution of the unit corresponds to extent of the early Cretaceous arc associated with hypothetical westward subduction (Niida and Kito, 1986). Among exploration boreholes, MITI Sorachi and MITI Nanporo (Fig. 2) confirmed igneous basements similar to the Kumaneshiri Group (Kato et al., 1990). Thus, the Ishikari lowland seems to be underlain by the Cretaceous igneous rocks, which extend to the Oshima belt of western Hokkaido (Fig. 1; Kato et al., 1990).

From the Oshima belt, Otofuji et al. (1994) reported Paleogene NRM directions with large westerly deflections, and interpreted that the belt belonged to northeast Japan rotated counterclockwise according to the back-arc spreading in the

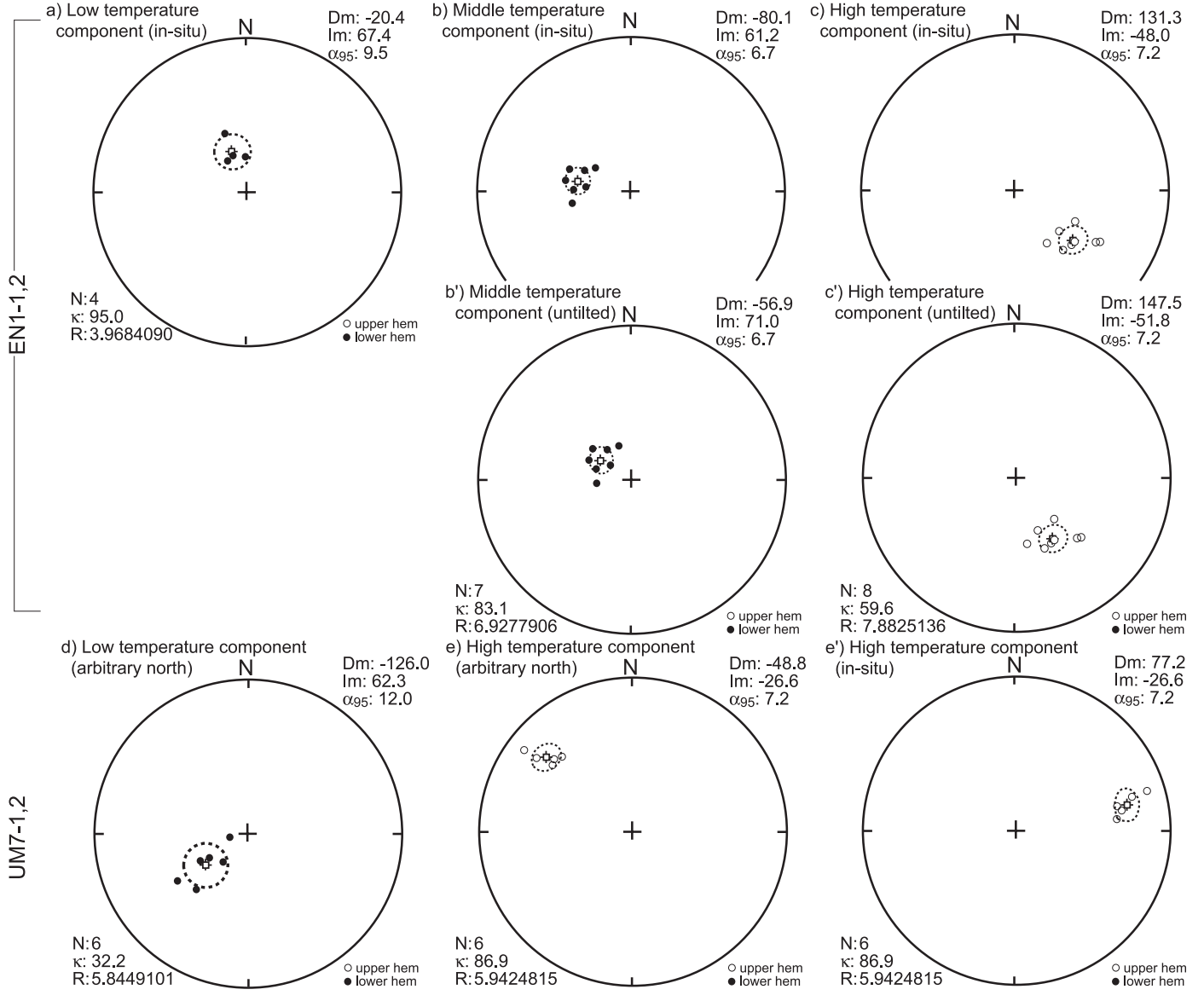

Fig. 8. Mean magnetic directions obtained from the Eniwa SK-1 (EN) and MITI Umaoi (UM) boreholes. Solid and open circles are on the lower and upper hemispheres of the equal-area projections, respectively. Dotted ovals are 95% confidence limits.

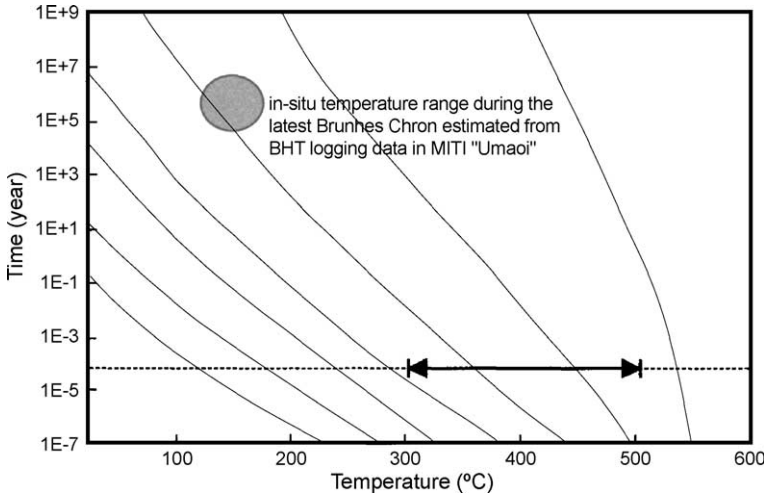

Fig. 9. Thermoviscous remagnetization contours (thin solid curves) after Middleton and Schmidt (1982) based on the SD relaxation theory (Walton, 1980). Shaded oval depicts plausible remagnetization temperatures reached in nature, estimated from the logging data of bottom-hole temperatures conducted on the MITI Umaoi (JNOC, 1997). Horizontal arrow shows the range of laboratory unblocking temperatures (T_{UB}) of "low-temperature component" residing in the UM core sample (gabbro).

Neogene. As shown in Table 3, the Cretaceous paleomagnetic data in our study area are characterized by westerly deflections, although quantitative evaluation is difficult for the small number of data with ambiguities in correction of tectonic tilting as stated in Section 4.4. Thus, the downthrown side of the floor thrust of the Hidaka collision front may be an extension of the Cretaceous igneous belt of northeast Japan.

5.2. Rotational deformation of the collision front

Surface paleomagnetic data obtained from southern central Hokkaido (Table 3; Kodama et al., 1993) is indicative of clockwise rotational motion. Considering ages of the measured rock units, clockwise rotation is assigned to the early to middle Miocene, and interpreted as a result of right-lateral shear (e.g., Lallemand and Jolivet, 1986; Kimura, 1996), which is postulated based on structural geology and tectonic framework. Late Oligocene to early Miocene right-lateral shear is detected on deformation of sedimentary rocks (Kusunoki and Kimura, 1998). Oblique collision between the North American (Okhotsk) and Eurasian Plates, and spreading of the Kuril Basin (Kusunoki and Kimura, 1998) are assumed cause of the transcurrent motion. Based on en echelon arrangement of anticlines of oil fields around MITI Karumai borehole (Fig. 2), Oka (1986) suggested that the wrench deformation had been lingering on the western flank of the Hidaka Collision Zone until the middle Miocene. Thus, long-standing right-lateral shearing is widely accepted as structural trend in southern central Hokkaido. Takeuchi et al. (1999) proposed a model of ball-bearing clockwise motions of whole lithosphere blocks (Fig. 1b).

Table 3
Paleomagnetic data reported from the southern central Hokkaido

Area/Well	Geologic age	Remarks	Declination (°)	Inclination (°)	α_{95} (°)	N
Yubari[a]	Oligocene–Miocene	E(U)	−155.0	−64.0	14.0	8
MITI Umaoi	Late Oligocene	E(U)	−45.8	40.9	25.2	4
Eniwa SK-1	Cretaceous	W(D)	147.5	−51.8	–	1
MITI Umaoi	Cretaceous	W(D)	77.2	−26.6	–	1

N is number of sites.

[a] Data from Kodama et al. (1993). W(D) and E(U) are western (downthrown) and eastern (upthrown) sides of the Umaoi Fault, respectively.

However, our Oligocene paleomagnetic data obtained from the MITI Umaoi show counterclockwise sense of rotations, opposite from the almost contemporaneous surface directions (Kodama et al., 1993). In spite of fairly large directional scatter (Table 3), comparison of the two data-sets indicates significant relative rotation of 70.8° with ΔR (Beck, 1980) of 47.9°. It is noted that both of these datasets belong to the eastern (upthrown) side of the floor thrust of the deformation front. Because single fault large enough to compensate the differential rotation has not been reported between these areas (see Fig. 2), the present result suggests more complicated rotational process in the transpressional deformation zone. Paleomagnetic interpretation linked with detail fault assessment based on structural geology is required, as attempted by Mino et al. (2001) for northeast Japan arc.

5.3. Recent E–W contraction on the collision front

Since the late Neogene, southern central Hokkaido has been a site of arc–arc collision as a result of westward migration of the Kuril fore-arc sliver (Fig. 1; Kimura and Tamaki, 1985; Kimura, 1996). Quaternary E–W contraction is detected on active fault distribution (Ikeda et al., 2002) and geodetic data (Tada and Kimura, 1987). Although the plate convergence history in larger scale and resultant mountain-building process in Hokkaido is not fully understood, the recent tectonic episode may enhance contraction and thrust activity on the deformation front.

In an effort to determine the duration of thrusting, we conducted a one-dimensional maturity modeling at the MITI Umaoi borehole for the downthrown rock unit of the floor thrust in Fig. 3 with the LLNL kinetic model (Sweeney and Burnham, 1990). Based on diatom assemblages of the growth strata (Kurita and Yokoi, 2000), oldest initiation of thrusting is assigned to ca. 11 Ma. Youngest initiation of the thrust is set at 2 Ma, since T_{UB} range of the TVRM component (Fig. 9) residing in the basement rock implies recent burial. For the both scenarios, maturity levels of organic matters are calculated based on burial histories of the downthrown block. Fig. 10 presents the results of modeling for the Eocene Poronai Formation together with measured maturity levels of vitrinite (%Ro). In the formation, maturity levels shown by %Ro rise as burial depth increases, which implies contamination from different horizons is not serious. Obviously, the youngest scenario accords with the maturation trends in nature. Therefore, we conclude that the E–W contraction along the collision front has been activated in the Quaternary. The continental collision

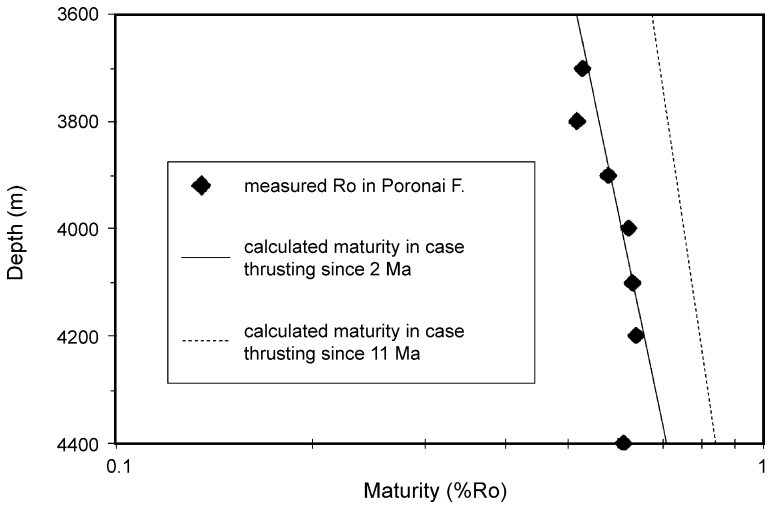

Fig. 10. Organic maturity levels of the Poronai Formation (Eocene) in the MITI Umaoi borehole. Vitrinite reflectance data (%Ro) measured on cuttings are shown by dots. Maturity levels calculated on the basis of a kinetic model are drawn as thin lines, which represent possible scenarios of thrusting of the Umaoi Fault and burial history of the downthrown-side block containing the geochemical sampling interval (MM in Fig. 3).

in central Hokkaido is an ongoing tectonic event with westward propagation.

6. Conclusions

(1) Downthrown block of the floor thrust of the arc–arc collision front in southern central Hokkaido is underlain by the Cretaceous igneous rocks extending to northeast Japan. Westerly deflections in ChRM directions of the subsurface Cretaceous samples may be related to counterclockwise rotation of northeast Japan during the Neogene back-arc opening.

(2) Rotational motion of the upthrown block is controversial. Late Oligocene Minami-naganuma Formation in the MITI Umaoi borehole consistently exhibits westerly deflections in untilted ChRM directions, whereas surface coeval samples have easterly deflected ChRM. A previous model of ball-bearing clockwise motions of crustal blocks cannot account for the reality. As a single fault, compensating such differential motions has not been reported, closer investigation on fault architecture and rotational motion is required to understand deformation mode of the arc–arc collision zone.

(3) Duration of the floor thrust activities of the collision front is estimated utilizing the maturity levels of organic matters in the downthrown block. Vitrinite reflectance trend of the Eocene Poronai Formation within the MITI Umaoi is best matched with a burial history assuming thrust activities since 2 Ma. Therefore, the E–W contraction along the collision front has been activated in the Quaternary.

Acknowledgements

The authors thank METI (Ministry of Economy, Trade and Industry, Japan), JNOC (Japan National Oil Corporation) and JAPEX for the permission to publish this work. We acknowledge the following persons: S. Yokoi for assistance during core sampling; H. Kurita for thoughtful discussion; N. Ishikawa for the use of paleomagnetic laboratory at Kyoto University. Reviews by R. Sutherland and an anonymous referee helped to improve this manuscript.

References

Arita, K., Toyoshima, T., Owada, M., Miyashita, S., Jolivet, L., 1986. Tectonic movements of the Hidaka metamorphic belt, Hokkaido, Japan. Monogr. Assoc. Geol. Collab. Jpn. 31, 247–263.

Beck Jr., M.E., 1980. Paleomagnetic record of plate-margin tectonic processes along the western edge of North America. J. Geophys. Res. 85, 7115–7131.

Geological Survey of Japan, 2002. Geological Maps of Japan 1:200,000 (Images) Ver. 2.0. Geological Survey of Japan, Tsukuba.

Ikeda, I., Komatsu, M., 1986. Early Cretaceous volcanic rocks of Rebun Island, north Hokkaido, Japan. Monogr. Assoc. Geol. Collab. Jpn. 31, 51–62.

Ikeda, Y., Imaizumi, T., Sato, H., Togo, M., Hirakawa, K., Miyauchi, T. (Eds.), 2002. Atlas of Quaternary Thrust Faults in Japan. University of Tokyo Press, Tokyo. 254 pp.

Ishiwada, Y., Aida, H., Atake, M., Araki, N., Iijima, A., Ikeda, A., Okuda, Y., Kikuchi, Y., Kojima, K., Saito, T., Sato, Y., Tanaka, S., Tono, S., Hirayama, J., Honza, E., Miyazaki, H., Morishima, H., Harada, Y., 1992. Oil and Natural Gas Resources in Japan. Natural Gas Exploration Association, Tokyo. 520 pp.

Ito, T., 2000. Crustal structure of the Hidaka collision zone and its foreland fold-and-thrust belt, Hokkaido, Japan. J. Jpn. Assoc. Pet. Technol. 65, 103–109.

JNOC (Japan National Oil Corporation), 1996. Report for the Offshore Geophysical Survey Iburioki-Senkaiiki, 1995 Fiscal Year. Japan National Oil Corporation, Tokyo, 35 pp.

JNOC (Japan National Oil Corporation), 1997. Report for the Geological Study of MITI Umaoi Borehole, 1996 Fiscal Year. Japan National Oil Corporation, Tokyo, 61 pp.

Kato, M., Katsui, Y., Kitagawa, Y., Matsui, M. (Eds.), 1990. Regional Geology of Japan: Part 1. Hokkaido. Kyoritsu Shuppan, Tokyo. 337 pp.

Katsumata, K., Wada, N., Kasahara, M., Okayama, M., Ichiyanagi, M., Ishikawa, H., Takada, M., Cho, I., Umino, N., Okada, T., Nakamura, A., Hori, S., Tachibana, K., Kono, T., Nida, K., Hashimoto, K., Ito, Y., Igarashi, T., Nakajima, J., Asano, Y., Ito, A., Uchida, N., Soda, Y., Ujikawa, H., Hasemi, A., Demachi, T., Hirata, N., Urabe, T., Sakai, S., Ide, S., Ogino, I., Seto, N., Sakai, K., Hashimoto, S., Haneda, T., Yamanaka, Y., Miura, K., Hagiwara, H., Kobayashi, M., Inoue, Y., Tagami, K., Nakagawa, S., Tsuda, K., Matsubara, M., Tada, T., Aoyama, H., Matsuzawa, T., Zhao, Y., Yamazaki, F., Yamada, M., Sasaki, Y., Hiramatsu, Y., Saiga, A., Komori, T., Umeda, Y., Ito, K., Koizumi, M., Wada, H., Hirano, N., Nishida, R., Matsushima, T., Uehira, K., Ooshima, M., Hirano, S., 2002. Distribution of hypocenters and focal mechanisms in and around the Hidaka arc–arc collision zone revealed by a dense temporary seismic network. Bull. Earthq. Res. Inst. 77, 199–223.

Kazuka, T., Kikuchi, S., Ito, T., 2002. Structure of the foreland fold-and-thrust belt, Hidaka Collision Zone, Hokkaido, Japan: re-

processing and re-interpretation of the JNOC seismic reflection profiles 'Hidaka' (H91-2 and H91-3). Bull. Earthq. Res. Inst. 77, 97–109.

Kikawa, E., 1993. Drilling-induced remanent magnetization in gabbroic drill cores. J. Jpn. Soc. Marine Surv. Technol. 5, 11–19.

Kimura, G., 1996. Collision orogeny at arc–arc junctions in the Japanese Islands. The Island Arc 5, 262–275.

Kimura, G., Tamaki, K., 1985. Tectonic framework of the Kuril arc since its initiation. In: Nasu, N., Uyeda, S., Kushiro, I., Kobayashi, K., Kagami, H. (Eds.), Formation of Active Ocean Margins. Terra Publishing, Tokyo, pp. 641–676.

Kirschvink, J.L., 1980. The least-squares line and plane and the analysis of palaeomagnetic data. Geophys. J. R. Astron. Soc. 62, 699–718.

Kodama, K., Takeuchi, T., Ozawa, T., 1993. Clockwise tectonic rotation of Tertiary sedimentary basins in central Hokkaido, northern Japan. Geology 21, 431–434.

Koike, K., Machida, H. (Eds.), 2001. Atlas of Quaternary Marine Terraces in the Japanese Islands. University of Tokyo Press, Tokyo. 105 pp. with three CD-ROMs and two oversize maps.

Komatsu, M., Miyashita, S., Maeda, J., Osanai, Y., Toyoshima, T., 1983. Disclosing of a deepest section of continental-type crust up-thrust as the final event of collision of arcs in Hokkaido, North Japan. In: Hashimoto, M., Uyeda, S. (Eds.), Accretion Tectonics in the Circum-Pacific Regions. Terra Publishing, Tokyo, pp. 149–165.

Komatsu, M., Osanai, Y., Toyoshima, T., Miyashita, S., 1989. Evolution of the Hidaka metamorphic belt, Northern Japan. In: Daly, J.S., Cliff, R.A., Yardley, B.W.D. (Eds.), Evolution of Metamorphic Belts. Geological Society, London, pp. 487–493.

Kurita, H., Yokoi, S., 2000. Cenozoic tectonic settings and a current exploration concept in southern central Hokkaido, northern Japan. J. Jpn. Assoc. Pet. Technol. 65, 58–70.

Kusunoki, K., Kimura, G., 1998. Collision and extrusion at the Kuril–Japan arc junction. Tectonics 17, 843–858.

Lallemand, S., Jolivet, L., 1986. Japan Sea: a pull-apart basin? Earth Planet. Sci. Lett. 76, 375–389.

Lowrie, W., 1990. Identification of ferromagnetic minerals in a rock by coercivity and unblocking temperature properties. Geophys. Res. Lett. 17, 159–162.

McFadden, P.L., McElhinny, M.W., 1988. The combined analysis of remagnetization circles and direct observations in palaeomagnetism. Earth Planet. Sci. Lett. 87, 161–172.

Middleton, M.F., Schmidt, P.W., 1982. Paleothermometry of the Sydney Basin. J. Geophys. Res. 87, 5351–5359.

Mino, K., Yamaji, A., Ishikawa, N., 2001. The block rotation in the Uetsu area, northern part of Niigata Prefecture, Japan. Earth Planets Space 53, 805–815.

Nagata, M., Kito, N., Niida, K., 1986. The Kumaneshiri Group in the Kabato Mountains: the age and nature as an Early Cretaceous volcanic arc. Monogr. Assoc. Geol. Collab. Jpn. 31, 63–79.

Niida, K., Kito, N., 1986. Cretaceous arc-trench systems in Hokkaido. Monogr. Assoc. Geol. Collab. Jpn. 31, 379–402.

Oda, H., Suzuki, H., 2000. Paleomagnetism of Triassic and Jurassic red bedded chert of the Inuyama area, central Japan. J. Geophys. Res. 105, 25743–25767.

Oka, T., 1986. Distribution and tectonic evolution of Late Cenozoic basins in Hokkaido. Monogr. Assoc. Geol. Collab. Jpn. 31, 295–320.

Otofuji, Y., Kambara, A., Matsuda, T., Nohda, S., 1994. Counter-clockwise rotation of Northeast Japan: paleomagnetic evidence for regional extent and timing of rotation. Earth Planet. Sci. Lett. 121, 503–518.

Shibuya, H., Sasajima, S., 1986. Paleomagnetism of red cherts: a case study in the Inuyama area, central Japan. J. Geophys. Res. 91, 14105–14116.

Suzuki, N., Kurita, H., Takashima, R., 1999. Earliest Cretaceous radiolarian assemblages from a deep borehole section in the southern Ishikari Plain, central Hokkaido, and their implications. Abstract of 106th Annual Meeting of the Geological Society of Japan. Geological Society of Japan, Tokyo, pp. 307.

Sweeney, J.J., Burnham, A.K., 1990. Evaluation of a simple model of vitrinite reflectance based on chemical kinetics. Am. Assoc. Pet. Geol. Bull. 74, 1559–1570.

Tada, T., Kimura, G., 1987. Collision tectonics and crustal deformation at the southwestern margin of the Kurile Arc. J. Seismol. Soc. Jpn. (Zisin) 40, 197–204.

Taketomi, H., Nishita, H., 2002. Petroleum system in the Ishikari–Hidaka sedimentary basin: Geochemical interpretation of the Yufutsu oil/gas field. J. Jpn. Assoc. Pet. Technol. 67, 52–61.

Takeuchi, T., Kodama, K., Ozawa, T., 1999. Paleomagnetic evidence for block rotations in central Hokkaido–south Sakhalin, Northeast Asia. Earth Planet. Sci. Lett. 169, 7–21.

Walton, D., 1980. Time-temperature relations in the magnetization of assemblies of single domain grains. Nature 286, 245–247.